Published in final edited form as:
Biomaterials. 2010 September ; 31(27): . doi:10.1016/j.biomaterials.2010.05.014.

The use of microfiber composites of elastin-like protein matrix reinforced with synthetic collagen in the design of vascular grafts

Jeffrey M. Caves[a,b,1], **Vivek A. Kumar**[a,b,1], **Adam W. Martinez**[a,b], **Jeong Kim**[c], **Carrie M. Ripberger**[c], **Carolyn A. Haller**[a], and **Elliot L. Chaikof**[a,b,c,*]

[a]Departments of Surgery, Emory University, Atlanta, GA, USA

[b]Biomedical Engineering, Emory University/Georgia Institute of Technology, Atlanta, GA 30332, USA

[c]School of Chemical and Biomolecular Engineering, Georgia Institute of Technology, Atlanta, GA 30322, USA

Abstract

Collagen and elastin networks contribute to highly specialized biomechanical responses in numerous tissues and species. Biomechanical properties such as modulus, elasticity, and strength ultimately affect tissue function and durability, as well as local cellular behavior. In the case of vascular bypass grafts, compliance at physiologic pressures is correlated with increased patency due to a reduction in anastomotic intimal hyerplasia. In this report, we combine extracellular matrix (ECM) protein analogues to yield multilamellar vascular grafts comprised of a recombinant elastin-like protein matrix reinforced with synthetic collagen microfibers. Structural analysis revealed that the fabrication scheme permits a range of fiber orientations and volume fractions, leading to tunable mechanical properties. Burst strengths of 239–2760 mm Hg, compliances of 2.8–8.4%/100 mm Hg, and suture retention strengths of 35–192 gf were observed. The design most closely approximating all target criteria displayed a burst strength of 1483 ± 43 mm Hg, a compliance of 5.1 ± 0.8%/100 mm Hg, and a suture retention strength of 173 ± 4 gf. These results indicate that through incorporation of reinforcing collagen microfibers, recombinant elastomeric protein-based biomaterials can play a significant role in load bearing tissue substitutes. We believe that similar composites can be incorporated into tissue engineering schemes that seek to integrate cells within the structure, prior to or after implantation in vivo.

Keywords

Elastin; Collagen; Mechanical properties; Fiber-reinforced composite; Vascular graft; Recombinant protein

1. Introduction

After decades of investigation, small to medium (≤4–≤7 mm) diameter prosthetic vascular grafts continue to occlude due to peri-anastomotic intimal hyperplasia, surface thrombogenicity, and failure to develop an endothelialized lumen. Intimal hyperplasia, the

*Corresponding author. Emory University, 101 Woodruff Circle, Rm 5105, Atlanta, GA 30322. Tel.: +1 404 727 8413; fax: +1 404 727 3660., echaiko@emory.edu (E.L. Chaikof).

[1]These authors contributed equally to these investigations.

formation of pannus tissue with luminal narrowing, is driven in part by endothelial injury and mechanical mismatch between stiff prosthetics and a compliant native artery. Disrupted flow and shear stresses are also recognized factors [1]. Vascular graft thrombogenicity results from protein and cell adsorption, thrombin and fibrin formation, and platelet activation and aggregation. Ongoing research to improve permanent implants, such as thromboresisant coatings [2], compliant non-degradable polymers [3,4], and advanced cell seeding [5], is increasingly complemented by progress in vascular tissue engineering.

Biomaterials adapted for vascular tissue engineering include animal-derived biopolymer gels such as collagen [6], fibrin [7–9], or composites [10]; biodegradable polymers such as polylactic acid, polyglutamic acid, polycaprolactone, polyurethanes, and their copolymers or composite structures [11–18]; and decellularized natural tissues [19–26]. The assembly of cell-populated haemodialysis access grafts from extracellular matrix (ECM) proteins secreted by autologous cells, with no foreign biomaterial, is currently one of the most advanced arterial tissue engineering technologies [27]. Nonetheless, many strategies remain hampered by prolonged in vitro culture times required by cells for the secretion of an organized, mechanically sound ECM. In addition, despite recent advances, elastin content is equivalent to levels in vein in the best instances, rather than approaching arterial compositions [7,9,17]. Due to these limitations, we have pursued technology consisting of scaffolds with controlled collagen–elastin ratios and structural orientation, fabricated without bioreactor culture.

Recombinant proteins derived from elastin sequences have been investigated as gels [28–30], films [31,32], micelles [33], or nanofibers [34,35] with potential applications in drug delivery [28,36,37], tissue engineering [38,39] or as components of implanted medical devices [40,41]. In particular, elastin-like protein triblock copolymers demonstrate fermentation yields of 200–700 mg/mL, with less contaminating endotoxin than clinical grade alginate [42]. These protein triblocks can be molded or laminated due to a defined inverse transition temperature, above which the hydrophobic endblocks of the copolymer aggregate to produce a physically crosslinked hydrogel [29]. Addition of amino groups at the block interfaces provides the capacity for covalent crosslinking [42]. Long-term stability has been observed in vivo under some conditions, even in the absence of covalent crosslinks [43]. Mechanical properties are tunable through adjustment of copolymer block size or sequence, or through implementation of processing conditions that alter the degree of microphase block mixing [30,35]. Primate ex vivo shunt studies have confirmed that elastin-like protein polymers can serve as thromboresistant luminal coatings for small diameter ePTFE vascular grafts [40].

Early vascular tissue engineering with collagen gels validated the concept of ECM protein scaffolds but lacked strength largely due to microstructural deviations from native collagen fibril orientation, architecture, and packing density [6]. To provide densely-packed, oriented collagen scaffolds, we developed a scalable spinning process for production of continuous microfiber composed of aligned, D-periodic collagen fibrils [44]. In addition, composites incorporating continuous, aligned, microcrimped collagen fiber architectures in an elastin-like protein matrix have recently been described [45].

We postulate that biologically inspired structures produced from synthetic or molecularly engineered collagen and elastin analogues, which recapitulate the biomechanical and biochemical features of the native extracellular matrix, provide an advanced foundation for engineering living tissue. As a case in point, this report describes the generation of an acellular arterial substitute consisting of a multi-lamellar structure formulated from integrated synthetic collagen microfibers and a recombinant elastin-like protein (Fig. 1). In addition to requiring new scalable approaches for producing resilient elastin analogues and

synthetic collagen fibers of high strength, different strategies were required for fabricating integrated structures that could be easily processed into a tubular geometry that displays tailored biomechanical responses. Given the non-thrombogenic features of the elastin analogue used in this approach [40], acellular constructs may well exhibit favorable performance characteristics as implanted vascular grafts. However, we believe this technology also provides an important framework for schemes driven either by ex vivo or in situ regeneration of tissue.

2. Materials and methods

2.1. Synthesis of a recombinant elastin-mimetic triblock protein polymer

Genetic engineering, expression, purification, and characterization of the elastin-mimetic protein polymer, designated *LysB10*, has been described elsewhere [42]. Briefly, the flanking 75 kDa endblocks of the protein polymer contained 33 repeats of the hydrophobic pentapeptide sequence $[IPAVG]_5$, and the central 58 kDa midblock consisted of 28 repeats of the elastic, hydrophilic sequence $[(VPGAG)_2VPGEG(VPGAG)_2]$. Additional sequences between blocks and at the C terminus include the residues [KAAK], which along with the N-terminal amine provide amino groups for chemical crosslinking.

The protein polymer sequence is contained in a single contiguous reading frame within the plasmid pET24-a, which was used to transform the *Escherichia coli* expression strain BL21(DE3). Fermentation was performed at 37 °C in Circle Grow (QBIOgene) medium supplemented with kanamycin (50 μg/mL) in a 100 L fermentor at the Bioexpression and Fermentation Facility of the University of Georgia-Athens. Cultures were incubated under antibiotic selection for 24 h at 37 °C. Isolation of the *LysB10* consisted of breaking the cells with freeze/thaw cycles and sonication, a high speed centrifugation (20,000 RCF, 40 min, 4 °C) with 0.5% poly(ethyleneimine) to precipitate nucleic acids, and a series of alternating warm/cold centrifugations. Each cold centrifugation (20,000 RCF, 40 min, 4 °C) was followed by the addition of NaCl to 2 M to precipitate the protein polymer as it incubated for 25 min at 25 °C. This was followed by warm centrifugation (9500 RCF, 15 min, 25) and resuspension of the pellet in cold, sterile PBS on ice for 10 to 20 min. After 6 to 10 cycles, when minimal contamination was recovered in the final cold centrifugation, the material was subject to a warm centrifugation, resuspended in cold sterile PBS, dialyzed, and lyophilized. Lyophilized protein was resuspended in sterile molecular grade water at 1 mg/mL and endotoxin levels were assessed according to manufacturer instructions using the Limulus Amoebocyte Lysate (LAL) assay (Cambrex). Levels of 0.1 EU/mg were obtained (1 EU = 100 pg of endotoxin), which corresponds to endotoxin levels for clinically used alginate (Pronova sodium alginate, endotoxin ≤100 EU/g).

2.2. Isolation and purification of monomeric collagen

Acid-soluble, monomeric rat-tail tendon collagen (MRTC) was obtained from Sprague–Dawley rat tails following Silver and Trelstad [46]. Frozen rat tails (Pel-Freez Biologicals, Rogers, AK) were thawed at room temperature and tendon was extracted with a wire stripper, immersed in 10 mM HCl (pH 2.0; 150 mL per tail) and stirred for 4 h at room temperature. Soluble collagen was separated by centrifugation at 30,000*g* and 4 °C for 30 min followed by sequential filtration through P8, 0.45 μm, and 0.2 μm membranes. Addition of concentrated NaCl in 10 mM HCl to a net salt concentration of 0.7 M, followed by 1 h stirring and 1 h centrifugation at 30,000*g* and 4 °C, precipitated the collagen. After overnight re-dissolution in 10 mM HCl the material was dialyzed against 20 mM phosphate buffer for at least 8 h at room temperature. Subsequent dialysis was performed against 20 mM phosphate buffer at 4 °C for at least 8 h and against 10 mM HCl at 4 °C overnight. The resulting MRTC solution was stored at 4 °C for the short-term or frozen and lyophilized.

2.3. Production of a synthetic collagen microfiber by continuous co-extrusion

Synthetic collagen fibers were produced continuously and in large scale using a lab scale automated fiber spinning system, described elsewhere [44]. Briefly, a collagen solution (5 mg/mL in 10 mM HCl) and wet spinning buffer (WSB: 10 wt% poly (ethylene glycol) M_w = 35,000, 4.14 mg/mL monobasic sodium phosphate, 12.1 mg/mL dibasic sodium phosphate, 6.86 mg/mL TES (N-tris (hydroxymethyl) methyl-2-aminoethane sulfonic acid sodium salt), 7.89 mg/mL sodium chloride, pH 8.0) were extruded with a dual syringe pump (Harvard Apparatus, Holliston, MA). The collagen solution emerged through a 0.4 mm inner-diameter spinneret into the center of a vertical tube (1.6 mm inner-diameter × 1 m long fluoropolymer tubing) at 0.08 mL/min. Wet spinning buffer simultaneously advanced through a bubble trap and down the fluoropolymer tube at a rate of 1.0 mL/min. As it exited the spinneret, the collagen coagulated into a gel-like fiber and traveled downward with the WSB stream.

Upon emergence from the fluoropolymer tube, the fiber entered a 2 m-long rinsing bath of 70% ethanol in water. Continuous fiber was collected by winding it out of the rinsing bath onto segments of a polyvinyl chloride (PVC) carrier cylinder that rotated and translated automatically. After spinning, the fiber was placed in fiber incubation buffer (FIB: 7.89 mg/mL sodium chloride, 4.26 mg/mL dibasic sodium phosphate, 10 mM Tris, pH = 7.4) at 37 °C for 48 h [47]. Fiber was incubated directly on the carrier cylinders, followed by rinsing in ddH20 for 15 min before drying and transferring the fiber onto a second cylinder under tension using an automated fiber collecting system.

2.4. Fabrication of a small diameter vascular graft

Synthetic collagen fibers were arranged into parallel arrays, embedded within a thin membrane of a recombinant elastin analogue, and rolled into multilayered tubes (Fig. 2). Synthetic collagen fiber was arrayed about a rectangular frame rotated by a DC gearmotor and translated by an automated linear actuator (Velmex, Inc, Bloomfied, NY). Rotation and translation speeds were adjusted to control fiber spacing. Fibers underwent vapor phase glutaraldehyde crosslinking by placement in a desiccator containing a 25% (w/v) glutaraldehyde solution for 24 h. Two fiber arrays were then transferred to a glass plate and secured with tape. A protractor beneath the plate was used to align the two arrays to a desired fiber angle or orientation.

Solutions of *LysB10* were prepared at 10-wt% concentration in ice-cold ddH_2O. Argon was bubbled through the solutions, followed by centrifugation at 4 °C and 500*g* for 5 min. To embed the fiber layouts, precision 130 μm thick plastic shims (Precision Brand, Inc., Downers Grove IL) were placed around the layouts, and all embedding materials cooled to 4 °C. The *LysB10* solution was distributed over the fibers and a sheet of polycarbonate was pressed on top of the solution. The fibers and the *LysB10* solution resided within the 130 μm space, sandwiched between the polycarbonate sheet and a glass plate that were separated by precision shims. Following incubated for 1 h at 4 °C, the embedding assembly was transferred to room temperature for 20 min for inverse transition temperature molding. The glass and polycarbonate were separated, affording a 100 μm thick fiber-reinforced protein polymer film, which was trimmed to yield a 5 × 8 cm membrane.

Membranes were rolled about a 4 mm diameter Teflon tube to form a 5 cm long, six-layer tube, which was wrapped in a thermoplastic film. The assembly was incubated at 4 °C overnight to promote interlayer bonding, and then centrifuged at 200*g* and 4 °C for 5 min to remove trapped air bubbles. The assembly was then incubated at 37 °C for 180 min, the thermoplastic wrap was removed, and constructs were hydrated in PBS at 37 °C for 30 min. All designs, except 2a, were then thermally annealed at 60 °C in PBS for 4 h. All constructs

were detached from the Teflon mandrel, crosslinked in PBS at 37 °C containing 0.5% (w/v) glutaraldehyde for 24 h and rinsed for 12 h in PBS.

2.5. Measurements of vascular graft fiber orientation, spacing and wall thickness

The spacing and orientation of the synthetic collagen fibers were measured from photographs of planar fiber arrays prior to embedding in protein polymer (Fig. 2, Table 1). Orientation was measured from digital photographs of the fiber layouts using the fast-Fourier transform tool from ImageJ software [48]. After completing vascular graft fabrication, samples were stained with Van Gieson for 5 min, rinsed, and photographed. Additionally, three rings were sectioned from each graft, photographed, and wall thickness measured at six points around the circumference of each ring.

2.6. Graft pressure-diameter responses and burst pressure

Vascular graft compliance and burst pressure were evaluated using a custom-built inflation system. Grafts were suspended vertically in 37 °C PBS, with the upper end connected by tubing to a syringe pump (Harvard Apparatus, Holliston, MA) and the lower end sealed and fastened to a 5 g weight. Grafts were inflated with PBS supplied by the syringe pump at 4 mL/min, and a 3CCD camera (Dage-MTI, Michagan City, IN) with a 10x macro video zoom lens (Edmund Optics, Barrington, NJ) recorded video at 30 frames per second. Pressure was recorded with a pressure transducer (WIKA, Lawrenceville, GA). A PC equipped with data and image acquisition cards (PCI-1405 and PCI-6220, National Instruments, Austin, TX) acquired the video and pressure data. A Labview program synchronized the video and pressure data. A computer program written in MATLAB quantified the initial graft outer diameter (D_0) and the inflated diameter (D) from every video frame and calculated the percent change in diameter (D/D_0) corresponding to each pressure measurement. Each graft was preconditioned with 20 inflations to 250 mm Hg and video taken of the 21st inflation. Grafts were then inflated to failure while video and pressure data was recorded. Compliance (C), the percent change in outer diameter (D/D_0) per 100 mm Hg of applied pressure, was calculated as:

$$C = 1/b \times 100 \quad (1)$$

where b is the slope of a line fit to the pressure vs. D/D_0 curve between 80 and 120 mm Hg.

2.7. Suture retention strength

Specimens with dimensions of 4 × 4 mm were cut from each graft and mounted in a dynamic mechanical thermal analyzer (DMTA V, Rheometric Scientific, Inc., Newcastle, DE) with a 15 N load cell in the inverted orientation, immersed in a jacketed beaker filled with PBS at 37 °C. Prolene suture (4-0) was passed through the each sample, 2 mm from the edge, and fastened to the actuating arm of the instrument. Suture was pulled parallel to the central axis of the graft at a rate of 1 mm/s and the maximum force measured before suture tear-out was recorded in grams-force (gf). Five to six samples from each design were tested and the data expressed as mean ± standard deviation.

2.8. Scanning electron microscopy

Samples for scanning electron microscopy were cut with a razor blade to expose the lumen and the cross-section of the graft wall. Samples were critical point dried (E3000, Energy Beam Sciences, Inc., East Granby, CT), sputter coated with gold (Emscope SC-500, Emitech, Kent, England), and imaged with a DS-150 F scanning electron microscope (Topcon Co., Tokyo, Japan) operated at 15 kV.

3. Results and discussion

3.1. Development of a fabrication scheme to create vascular graft composites with controlled fiber orientation and spacing

The fabrication scheme facilitated the generation of vascular grafts of varying fiber content and architecture (Fig. 2). Table 1 summarizes the fiber spacing and orientation in the various graft designs. Although the angle and spacing measured from the fiber layout are close to the nominal values, photographs of the stained prototypes did suggest variability in the final fiber arrangement (Fig. 3). Variance in fiber layout may have been introduced through initial swelling of films, stretching of films while rolling onto the mandrel, or shrinkage of the structure during thermal annealing.

Several technologies have been explored in fabricating a small diameter vascular graft to optimize both strength and compliance, including filament winding, electrospinning, molding, and sheet wrapping. Filament winding, in which a filament is wrapped about a rotating, translating inner mandrel, allows the compliance and strength of the graft to be adjusted by modulation of the filament angle and density [49,50]. Like conventional textile grafts, a filament wound structure is permeable and must be filled or coated with a second material. Significantly, as the diameter of a filament wound graft expands under pulsatile flow, it may contract axially, repeatedly stressing the anastomosis sites [51]. Balancing high radial compliance and axial kink resistance with wound filament structures presents a challenge because circumferentially oriented fibers prevent kinking but restrict compliance, while axially aligned fibers have the opposite effect [49].

Experimental vascular grafts have also been created by electrospinning onto a rotating, translating mandrel. Fiber orientation may be achieved through strategies related to controlling the velocity of the electrospinning target or shaping the electric field [52]. In principle, adjustment of fiber orientation should allow control over graft compliance, similar to filament winding. Electrospun tubes have also been reinforced with wound filament, increasing burst strength [53]. Depending upon processing conditions, electrospinning can be slow and result in loss of material, even with multi-jet spinning heads [54]. We, and others, have electrospun elastin or elastin-mimetic recombinant proteins to serve as one element in an arterial substitute [35,53,55–58]. However, collagen has not been electrospun without the use of solvents that denature the protein [59]. Collagen may be blended with synthetic polymers or biopolymers and electrospun from non-denaturing solvents. However, it is unlikely that, upon degradation or loss of the non-collagen component, continuous uniform fibers will be produced with the strength of native collagen fibers [57,60].

Synthetic polymers and some biopolymers, such as collagen and fibrin can be molded into tubular structures. Compliance and strength of molded structures has been modulated by controlling the orientation of fibril networks that develops during the molding process [61] and through use of excimer laser ablation to generate arrays of pores [62]. The desired combination of compliance and strength can also be tuned by surrounding a soft, elastic tube with one or more stiffer tubes [63].

Sheet wrapping approaches are required for grafts fabricated from flat materials such as cell layers [64] and porcine small intestinal submusoca (SIS) sheets. This technique provides the opportunity to apply a variety of 2D fabrication techniques, and mimic the laminar structure of the native vessel wall. Automated wrapping devices may increase control and repeatability in these constructs [65]. Tubular elastin scaffolds, extracted from porcine carotid arteries, have been wrapped with SIS sheets [66]. The SIS wrap enhanced burst pressure and suture retention, and the compliance of the structure was visually similar to native artery under pulsatile conditions.

The fabrication scheme in this report combines aspects of filament winding and sheet wrapping. As a result, fiber layout can be adjusted to tune the mechanics of the composite structure. In addition, modified versions of this scheme should allow cells or growth factors to be distributed throughout the wall of the graft at spatially defined compositions.

3.2. Fiber architecture and elastin properties dictate the mechanical behavior of composite vascular grafts

Mechanical responses, including burst pressure, compliance, and suture retention strength are summarized in Table 1. Representative burst data is illustrated in Fig. 4, and the relationship between mechanical behavior of the vascular graft and fiber orientation and spacing is presented in Fig. 5. Thermal annealing enhanced burst pressure and suture retention while reducing compliance, consistent with prior observations that thermal annealing can increase the strength and Young's modulus of this protein polymer [67]. The magnitude of the thermal annealing effect demonstrates that the mechanical behavior of the elastin component strongly influenced the composite mechanics and burst pressure. In addition, collagen fiber orientation and spacing played a major role. At a fixed fiber orientation (30°), decreasing average fiber spacing led to increased fiber density with enhanced burst pressure and suture retention, but lower overall compliance. Likewise, with fiber spacing fixed and fiber angle increased, burst pressure and suture retention increased, but compliance decreased. Arterial substitutes matching native compliance levels may display less intimal hyperplasia and lead to increased graft patency [68–70]. Notably, arterial compliance varies broadly with age, sex, diet, smoking, and position in the vascular tree, ranging between 3 and 25%/100 mm-Hg [71,72]. This range highlights the advantage of platforms with the capacity to tailor compliance. Design 6 approaches the compliance of native arteries (Table 1). Given the trade-offs of thermal annealing, fiber orientation, and fiber spacing, a conduit with a fiber orientation of 22.5° and volume fraction of 7.3% (Design 6), was the closest overall match for target mechanical properties.

Burst pressures of native vein and artery (2000–3000+ mm-Hg) are often cited as benchmarks for bypass grafts, although blood pressure rarely exceeds 240 mm Hg. The high strength of native vessel may reflect a proxy measurement of fatigue resistance in the face of hypertension or other biochemical factors that contribute to arteriosclerosis or aneurysm formation. In the case of bypass grafts, high burst strength suggests a greater resistance to damage from suture-line stress, biaxial stress, and fatigue. Grafts designed to biodegrade and remodel may require greater burst strength to compensate for anticipated structural alterations. Here, we selected 1000 mm Hg as a target, well above physiologic conditions, in consideration of data demonstrating the stability of a physically crosslinked elastin-mimetic triblock protein polymer even in the absence of chemical crosslinks [43].

4. Conclusions

In this report we describe a process for the fabrication of vascular grafts from a recombinant elastin-like protein reinforced with collagen microfiber and assess the structural and mechanical properties of a series of prototypes. The process facilitated control over collagen microfiber orientation and density. In turn, fiber architecture and processing of the elastin-like protein modulated the suture retention strength, burst strength, and compliance. Iterative adjustments to the fiber layout led to a design that meets mechanical targets. The fabrication scheme employs a non-thrombogenic elastin-like protein with the possibility that these structures may be advantageous as vascular graft implants without further modification. In addition, modification of the scheme to incorporate living cells ex vivo or in situ may be feasible.

Acknowledgments

We gratefully acknowledge Wensheng Li for protein polymer purification. Supported by grants from the NIH and NSF.

References

1. Zilla P, Bezuidenhout D, Human P. Prosthetic vascular grafts: wrong models, wrong questions and no healing. Biomaterials. 2007; 28:5009–27. [PubMed: 17688939]
2. Jordan SW, Chaikof EL. Novel thromboresistant materials. J Vasc Surg. 2007; 45 (Suppl A):A104–15. [PubMed: 17544031]
3. Kannan RY, Salacinski HJ, Odlyha M, Butler PE, Seifalian AM. The degradative resistance of polyhedral oligomeric silsesquioxane nanocore integrated polyurethanes: an in vitro study. Biomaterials. 2006; 27:1971–9. [PubMed: 16253324]
4. Seifalian AM, Salacinski HJ, Tiwari A, Edwards A, Bowald S, Hamilton G. In vivo biostability of a poly(carbonate-urea)urethane graft. Biomaterials. 2003; 24:2549–57. [PubMed: 12695082]
5. Sreerekha PR, Krishnan LK. Cultivation of endothelial progenitor cells on fibrin matrix and layering on dacron/polytetrafluoroethylene vascular grafts. Artif Organs. 2006; 30:242–9. [PubMed: 16643382]
6. Weinberg CB, Bell E. A blood vessel model constructed from collagen and cultured vascular cells. Science. 1986; 231:397–400. [PubMed: 2934816]
7. Swartz DD, Russell JA, Andreadis ST. Engineering of fibrin-based functional and implantable small-diameter blood vessels. Am J Physiol Heart Circ Physiol. 2005; 288:H1451–60. [PubMed: 15486037]
8. Yao L, Liu J, Andreadis ST. Composite fibrin scaffolds increase mechanical strength and preserve contractility of tissue engineered blood vessels. Pharm Res. 2008; 25:1212–21. [PubMed: 18092140]
9. Liu JY, Swartz DD, Peng HF, Gugino SF, Russell JA, Andreadis ST. Functional tissue-engineered blood vessels from bone marrow progenitor cells. Cardiovasc Res. 2007; 75:618–28. [PubMed: 17512920]
10. Cummings CL, Gawlitta D, Nerem RM, Stegemann JP. Properties of engineered vascular constructs made from collagen, fibrin, and collagen-fibrin mixtures. Biomaterials. 2004; 25:3699–706. [PubMed: 15020145]
11. Niklason LE, Gao J, Abbott WM, Hirschi KK, Houser S, Marini R, et al. Functional arteries grown in vitro. Science. 1999; 284:489–93. [PubMed: 10205057]
12. Soletti L, Hong Y, Guan J, Stankus JJ, El-Kurdi MS, Wagner WR, et al. A bilayered elastomeric scaffold for tissue engineering of small diameter vascular grafts. Acta Biomater. 2009
13. Pektok E, Nottelet B, Tille JC, Gurny R, Kalangos A, Moeller M, et al. Degradation and healing characteristics of small-diameter poly(epsilon-caprolactone) vascular grafts in the rat systemic arterial circulation. Circulation. 2008; 118:2563–70. [PubMed: 19029464]
14. Stekelenburg M, Rutten MC, Snoeckx LH, Baaijens FP. Dynamic straining combined with fibrin gel cell seeding improves strength of tissue-engineered small-diameter vascular grafts. Tissue Eng Part A. 2009; 15:1081–9. [PubMed: 18831688]
15. Zhang L, Zhou J, Lu Q, Wei Y, Hu S. A novel small-diameter vascular graft: in vivo behavior of biodegradable three-layered tubular scaffolds. Biotechnol Bioeng. 2008; 99:1007–15. [PubMed: 17705246]
16. He W, Ma Z, Teo WE, Dong YX, Robless PA, Lim TC, et al. Tubular nanofiber scaffolds for tissue engineered small-diameter vascular grafts. J Biomed Mater Res A. 2009; 90:205–16. [PubMed: 18491396]
17. Iwasaki K, Kojima K, Kodama S, Paz AC, Chambers M, Umezu M, et al. Bio-engineered three-layered robust and elastic artery using hemodynamically-equivalent pulsatile bioreactor. Circulation. 2008; 118:S52–7. [PubMed: 18824769]

18. Shin'oka T, Matsumura G, Hibino N, Naito Y, Watanabe M, Konuma T, et al. Midterm clinical result of tissue-engineered vascular autografts seeded with autologous bone marrow cells. J Thorac Cardiovasc Surg. 2005; 129:1330–8. [PubMed: 15942574]
19. Derham C, Yow H, Ingram J, Fisher J, Ingham E, Korrosis SA, et al. Tissue engineering small-diameter vascular grafts: preparation of a biocompatible porcine ureteric scaffold. Tissue Eng Part A. 2008; 14:1871–82. [PubMed: 18950273]
20. Spark JI, Yeluri S, Derham C, Wong YT, Leitch D. Incomplete cellular depopulation may explain the high failure rate of bovine ureteric grafts. Br J Surg. 2008; 95:582–5. [PubMed: 18344206]
21. Gui L, Muto A, Chan SA, Breuer CK, Niklason LE. Development of decellularized human umbilical arteries as small-diameter vascular grafts. Tissue Eng Part A. 2009; 15:2665–76. [PubMed: 19207043]
22. Wengerter K, Dardik H. Biological vascular grafts. Semin Vasc Surg. 1999; 12:46–51. [PubMed: 10100385]
23. Sciacca V, Walter G, Becker HM. Biogenic grafts in arterial surgery–long-term results (I. The homologous vein–II. The modified heterologous bovine carotid artery–III. The human umbilical vein). Thorac Cardiovasc Surg. 1984; 32:157–64. [PubMed: 6206595]
24. Dardik H. The second decade of experience with the umbilical vein graft for lower-limb revascularization. Cardiovasc Surg. 1995; 3:265–9. [PubMed: 7655839]
25. Rosenburg N, Martinez A, Sawyer P, Wesolowski S, Postlewait R, Dillon M. Tanned collagen arterial prosthesis of bovine carotid origin in man. Preliminary studies of enzyme-treated heterografts. Ann Surg. 1966; 164:247–56. [PubMed: 5950359]
26. Hurt AV, Batello-Cruz M, Skipper BJ, Teaf SR, Sterling WA Jr. Bovine carotid artery heterografts versus polytetrafluoroethylene grafts. A prospective, randomized study. Am J Surg. 1983; 146:844–7. [PubMed: 6650773]
27. McAllister TN, Maruszewski M, Garrido SA, Wystrychowski W, Dusserre N, Marini A, et al. Effectiveness of haemodialysis access with an autologous tissue-engineered vascular graft: a multicentre cohort study. Lancet. 2009; 373:1440–6. [PubMed: 19394535]
28. Wright ER, Conticello VP. Self-assembly of block copolymers derived from elastin-mimetic polypeptide sequences. Adv Drug Deliv Rev. 2002; 54:1057–73. [PubMed: 12384307]
29. Wright E, McMillan R, Cooper A, Apkarian RP, Conticello VP. Thermoplastic elastomer hydrogels via self-assembly of an elastim-mimetic triblock polypeptide. Adv Funct Mater. 2002; 12:149–54.
30. Nagapudi K, Brinkman W, Leisen J, Thomas B, Wright E, Haller C, et al. Protein-based thermoplastic elastomers. Macromolecules. 2005; 38:345–54.
31. Wu X, Sallach R, Haller CA, Caves JA, Nagapudi K, Conticello VP, et al. Alterations in physical cross-linking modulate mechanical properties of two-phase protein polymer networks. Biomacromolecules. 2005; 6:3037–44. [PubMed: 16283724]
32. Wu X, Sallach RE, Caves JM, Conticello VP, Chaikof EL. Deformation responses of a physically cross-linked high molecular weight elastin-like protein polymer. Biomacromolecules. 2008; 9:1787–94. [PubMed: 18558738]
33. Sallach RE, Wei M, Biswas N, Conticello VP, Lecommandoux S, Dluhy RA, et al. Micelle density regulated by a reversible switch of protein secondary structure. J Am Chem Soc. 2006; 128:12014–9. [PubMed: 16953644]
34. Nagapudi K, Brinkman WT, Leisen JE, Huang L, McMillan RA, Apkarian RP, et al. Photomediated solid-state cross-linking of an elastin-mimetic recombinant protein polymer. Macromolecules. 2002; 35:1730–7.
35. Nagapudi K, Brinkman WT, Thomas BS, Park JO, Srinivasarao M, Wright E, et al. Viscoelastic and mechanical behavior of recombinant protein elastomers. Biomaterials. 2005; 26:4695–706. [PubMed: 15763249]
36. Herrero-Vanrell R, Rincon AC, Alonso M, Reboto V, Molina-Martinez IT, Rodriguez-Cabello JC. Self-assembled particles of an elastin-like polymer as vehicles for controlled drug release. J Control Release. 2005; 102:113–22. [PubMed: 15653138]

37. Dreher MR, Raucher D, Balu N, Michael Colvin O, Ludeman SM, Chilkoti A. Evaluation of an elastin-like polypeptide-doxorubicin conjugate for cancer therapy. J Control Release. 2003; 91:31–43. [PubMed: 12932635]
38. Liu JC, Heilshorn SC, Tirrell DA. Comparative cell response to artificial extra-cellular matrix proteins containing the RGD and CS5 cell-binding domains. Biomacromolecules. 2004; 5:497–504. [PubMed: 15003012]
39. Richman GP, Tirrell DA, Asthagiri AR. Quantitatively distinct requirements for signaling-competent cell spreading on engineered versus natural adhesion ligands. J Control Release. 2005; 101:3–12. [PubMed: 15588889]
40. Jordan SW, Haller CA, Sallach RE, Apkarian RP, Hanson SR, Chaikof EL. The effect of a recombinant elastin-mimetic coating of an ePTFE prosthesis on acute thrombogenicity in a baboon arteriovenous shunt. Biomaterials. 2007; 28:1191–7. [PubMed: 17087991]
41. Woodhouse KA, Klement P, Chen V, Gorbet MB, Keeley FW, Stahl R, et al. Investigation of recombinant human elastin polypeptides as non-thrombogenic coatings. Biomaterials. 2004; 25:4543–53. [PubMed: 15120499]
42. Sallach RE, Cui W, Wen J, Martinez A, Conticello VP, Chaikof EL. Elastin-mimetic protein polymers capable of physical and chemical crosslinking. Biomaterials. 2009; 30:409–22. [PubMed: 18954902]
43. Sallach RE, Cui W, Balderrama F, Martinez AW, Wen J, Haller CA, et al. Long-term biostability of self-assembling protein polymers in the absence of covalent crosslinking. Biomaterials. 2009
44. Caves JM, Kumar VA, Wen J, Cui W, Martinez A, Apkarian R, et al. Fibrillo-genesis in continuously spun synthetic collagen fiber. J Biomed Mater Res B Appl Biomater. 2010; 93:24–38. [PubMed: 20024969]
45. Caves JM, Kumar VA, Xu W, Naik N, Allen MG, Chaikof EL. Microcrimped collagen fiber-elastin composites. Adv Mater. 2010; 22:2041–4. [PubMed: 20544890]
46. Silver FH, Trelstad RL. Type I collagen in solution-structure and properties of fibril fragments. J Biol Chem. 1980; 255:9427–33. [PubMed: 7410433]
47. Pins GP, Christiansen DL, Patel R, Silver FH. Self-assembly of collagen fibers. Influence of fibrillar alignment and decorin on mechanical properties. Biophys J. 1997; 73:2164–72. [PubMed: 9336212]
48. Abramoff M, Magelhaes P, Ram S. Image processing with ImageJ. Biophotonics Int. 2004; 11:36–42.
49. Leidner J, Wong EW, MacGregor DC, Wilson GJ. A novel process for the manufacturing of porous grafts: process description and product evaluation. J Biomed Mater Res. 1983; 17:229–47. [PubMed: 6841365]
50. Hellener G, Cohn D, Marom G. Elastic response of filament wound arterial prostheses under internal pressure. Biomaterials. 1994; 15:1115–21. [PubMed: 7893913]
51. Sabelman, E. Biology, biotechnology, and biocompatibility of collagen. In: Williams, D., editor. Biocompatibility of tissue analogues. Boca Raton, FL: CRC Press; 1985. p. 27-66.
52. Teo W, Ramakrishna S. A review on electrospinning design and nanofibre assemblies. Nanotechnology. 2006; 17:R89–106. [PubMed: 19661572]
53. Smith MJ, McClure MJ, Sell SA, Barnes CP, Walpoth BH, Simpson DG, et al. Suture-reinforced electrospun polydioxanone-elastin small-diameter tubes for use in vascular tissue engineering: a feasibility study. Acta Biomater. 2008; 4:58–66. [PubMed: 17897890]
54. Tomaszewski W, Szadkowski M. Investigation of electrospinning with the use of a multi-jet electrospinning head. Fibres Text East Eur. 2005; 13:22–6.
55. Li M, Mondrinos MJ, Chen X, Gandhi MR, Ko FK, Lelkes PI. Co-electrospun poly (lactide-co-glycolide), gelatin, and elastin blends for tissue engineering scaffolds. J Biomed Mater Res A. 2006; 79:963–73. [PubMed: 16948146]
56. Buttafoco L, Kolkman NG, Poot AA, Dijkstra PJ, Vermes I, Feijen J. Electro-spinning collagen and elastin for tissue engineering small diameter blood vessels. J Control Release. 2005; 101:322–4. [PubMed: 15719516]

57. Buttafoco L, Kolkman NG, Engbers-Buijtenhuijs P, Poot AA, Dijkstra PJ, Vermes I, et al. Electrospinning of collagen and elastin for tissue engineering applications. Biomaterials. 2006; 27:724–34. [PubMed: 16111744]
58. Sell SA, McClure MJ, Barnes CP, Knapp DC, Walpoth BH, Simpson DG, et al. Electrospun polydioxanone-elastin blends: potential for bioresorbable vascular grafts. Biomed Mater. 2006; 1:72–80. [PubMed: 18460759]
59. Zeugolis DI, Khew ST, Yew ES, Ekaputra AK, Tong YW, Yung LY, et al. Electro-spinning of pure collagen nanofibres – just an expensive way to make gelatin? Biomaterials. 2008; 29:2293–305. [PubMed: 18313748]
60. Huang L, Nagapudi K, Apkarian RP, Chaikof EL. Engineered collagen-PEO nanofibers and fabrics. J Biomater Sci Polym Ed. 2001; 12:979–93. [PubMed: 11787524]
61. Barocas VH, Girton TS, Tranquillo RT. Engineered alignment in media equivalents: magnetic prealignment and mandrel compaction. J Biomech Eng. 1998; 120:660–6. [PubMed: 10412446]
62. Doi K, Nakayama Y, Matsuda T. Novel compliant and tissue-permeable microporous polyurethane vascular prosthesis fabricated using an excimer laser ablation technique. J Biomed Mater Res. 1996; 31:27–33. [PubMed: 8731146]
63. Sonoda H, Takamizawa K, Nakayama Y, Yasui H, Matsuda T. Coaxial double-tubular compliant arterial graft prosthesis: time-dependent morphogenesis and compliance changes after implantation. J Biomed Mater Res A. 2003; 65:170–81. [PubMed: 12734809]
64. L'Heureux N, Paquet S, Labbe R, Germain L, Auger FA. A completely biological tissue-engineered human blood vessel. FASEB J. 1998; 12:47–56. [PubMed: 9438410]
65. Kubo H, Shimizu T, Yamato M, Fujimoto T, Okano T. Creation of myocardial tubes using cardiomyocyte sheets and an in vitro cell sheet-wrapping device. Biomaterials. 2007; 28:3508–16. [PubMed: 17482255]
66. Hinds MT, Rowe RC, Ren Z, Teach J, Wu PC, Kirkpatrick SJ, et al. Development of a reinforced porcine elastin composite vascular scaffold. J Biomed Mater Res A. 2006; 77:458–69. [PubMed: 16453334]
67. Sallach RE, Leisen J, Caves JM, Fotovich E, Apkarian RP, Conticello VP, et al. A permanent change in protein mechanical responses can be produced by thermally induced microdomain mixing. J Biomater Sci Polym Ed. 2009; 20:1629–44. [PubMed: 19619402]
68. Bassiouny HS, White S, Glagov S, Choi E, Giddens DP, Zarins CK. Anastomotic intimal hyperplasia: mechanical injury or flow induced. J Vasc Surg. 1992; 15:708–16. discussion 16–7. [PubMed: 1560562]
69. Zarins CK, Giddens DP. Relationship between anastomotic hemodynamics and intimal thickening. J Vasc Surg. 1991; 13:738–40. [PubMed: 2027221]
70. Sottiurai VS, Yao JS, Batson RC, Sue SL, Jones R, Nakamura YA. Distal anastomotic intimal hyperplasia: histopathologic character and biogenesis. Ann Vasc Surg. 1989; 3:26–33. [PubMed: 2713229]
71. Hayoz D, Rutschmann B, Perret F, Niederberger M, Tardy Y, Mooser V, et al. Conduit artery compliance and distensibility are not necessarily reduced in hypertension. Hypertension. 1992; 20:1–6. [PubMed: 1618544]
72. Juonala M, Jarvisalo MJ, Maki-Torkko N, Kahonen M, Viikari JS, Raitakari OT. Risk factors identified in childhood and decreased carotid artery elasticity in adulthood: the Cardiovascular Risk in Young Finns Study. Circulation. 2005; 112:1486–93. [PubMed: 16129802]

Appendix

Figures with essential color discrimination. Figs. 1–3 in this article are difficult to interpret in black and white. The full color images can be found in the on-line version, at doi:10.1016/j.biomaterials.2010.05.014.

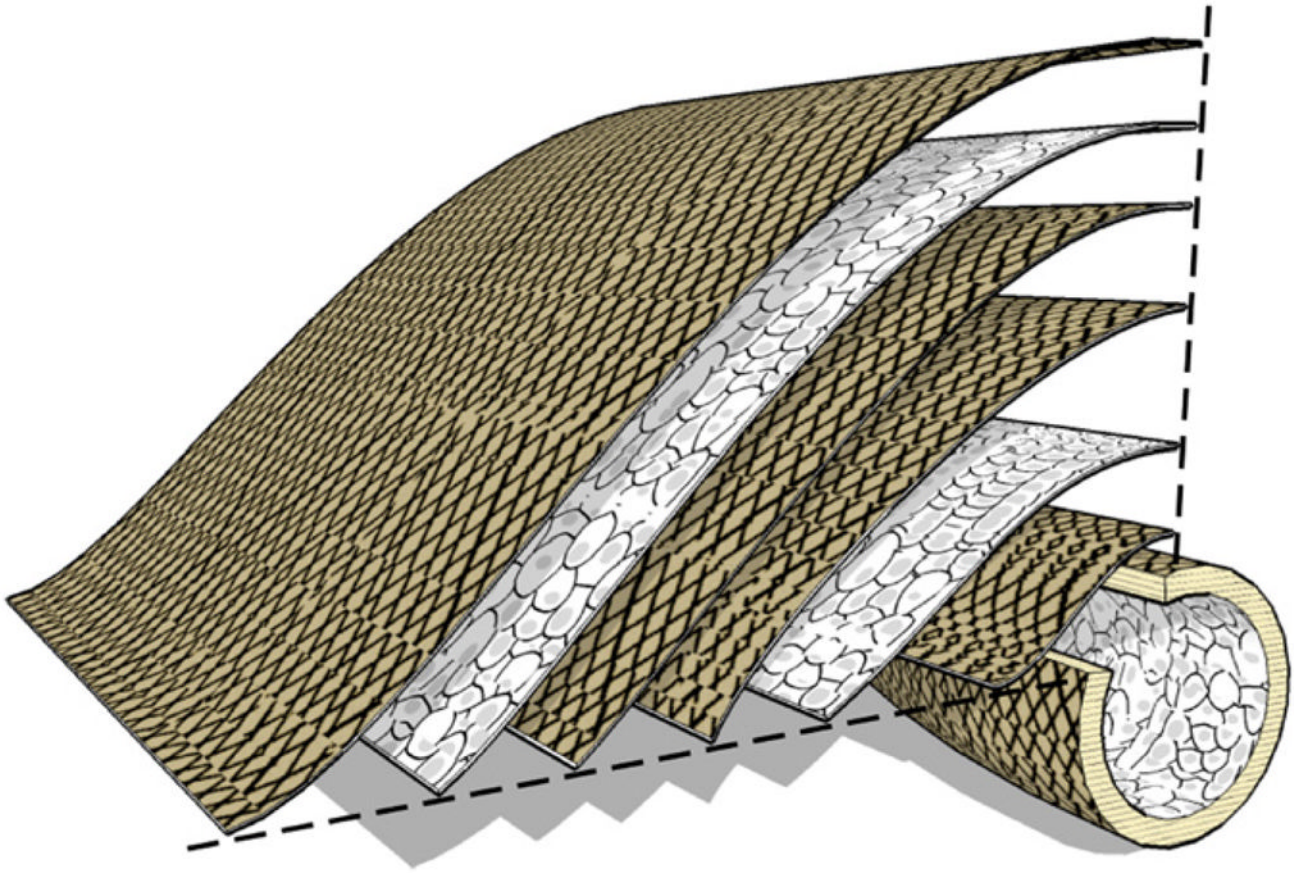

Fig. 1.

Multilamellar protein polymer microfiber composite vascular graft. The vessel wall consists of several layers (thickness 100 μm) of collagen microfiber embedded in protein polymer, with orientation and density established to attain mechanical design targets. Multilamellar structure may permit cell sheet or therapeutic integration at defined intervals.

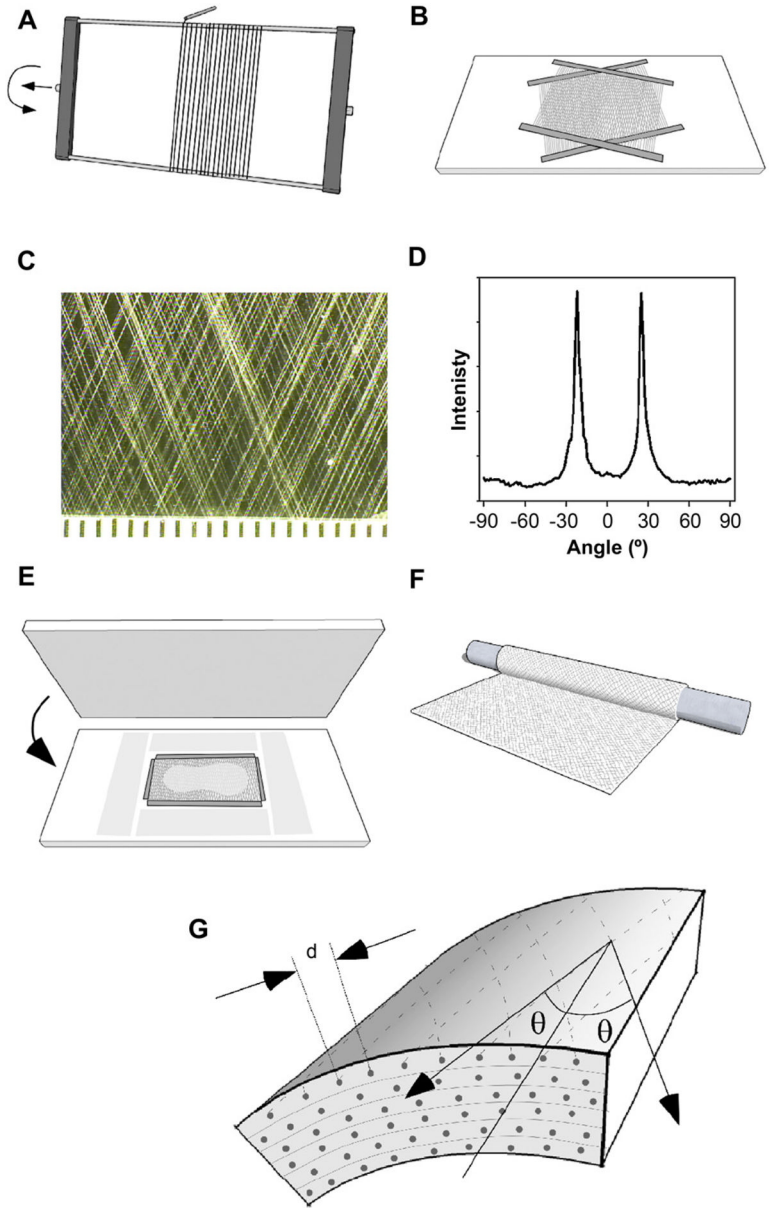

Fig. 2.

Fabrication of a fiber-reinforced small diameter vascular graft from oriented synthetic collagen microfiber arrays embedded in an elastin protein polymer matrix. (A) Parallel arrays of fiber were created by winding about a frame. (B) Two arrays were transferred to a glass sheet, positioned at the desired angle. (C) Average fiber spacing and orientation were characterized from digital photographs. (D) Fast Fourier transform analysis of fiber orientation. (E) Fibers were surrounded with precision-thickness shims and a solution of elastin protein polymer was applied before a polycarbonate sheet was pressed over the fibers to spread the solution into a thin film. Films were gelled by inverse transition temperature molding. (F) The gelled film was rolled about a Teflon rod to create a six-layered tube, bonded by inverse transition temperature lamination. (G) Schematic illustrates average fiber spacing (d) and angle (θ).

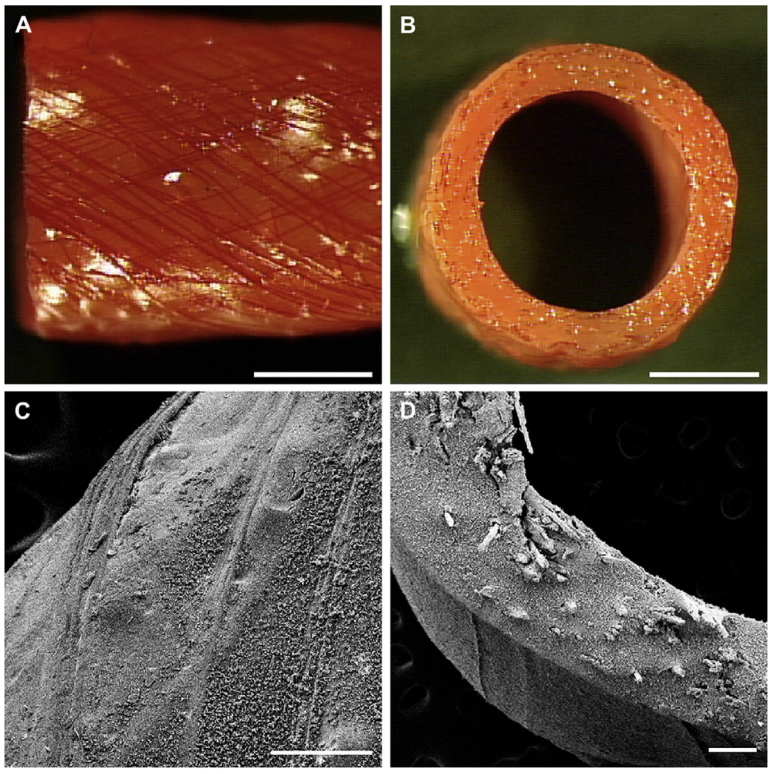

Fig. 3.

Photographs of the exterior (A) and cross-section (B) of grafts fabricated with a 30° collagen microfiber layouts. Collagen fibers are stained red with Van Gieson's stain. Scale bar 2 mm. Scanning electron microscopy of a prototype of design 6, exterior (C) and cross-section (D). Scale bar 200 μm.

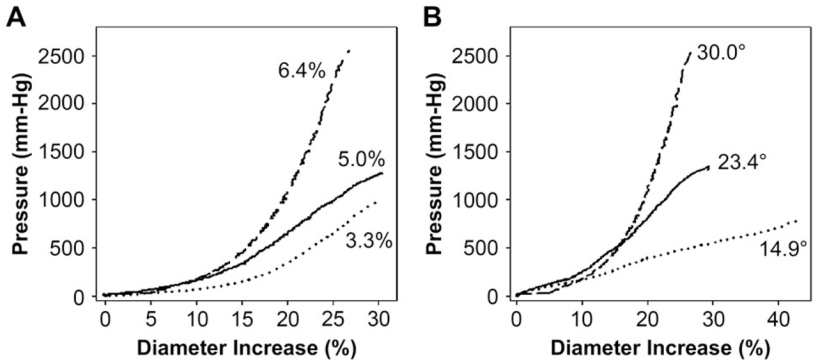

Fig. 4.

Representative pressure-diameter responses for composite vascular grafts. (A) Increasing fiber density at a fixed 30° fiber angle yielded prototypes with enhanced burst pressure. (B) Increasing fiber angle at a fixed fiber fraction of 6–7% yielded prototypes with decreased compliance.

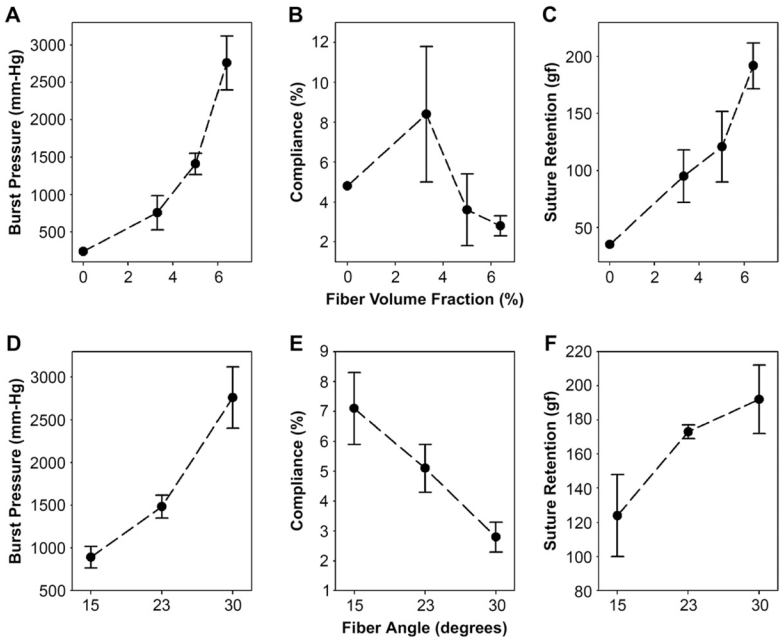

Fig. 5.

Dependence of burst strength, suture retention strength, and compliance on fiber spacing (A, B, C) and angle (D, E, F). Data represents means and standard deviations from at least three prototypes, except for the design with 0% fiber volume fraction, which was prototyped once.

Table 1

Structural and mechanical properties of graft prototyes.

Design number	Fiber spacing (nominal, mm)	Fiber fraction (%)	Fiber orientation (nominal, °)	Fiber orientation (measured, °)	Burst pressure (mm Hg)	Compliance (%/100 mm Hg)	Suture retention (gf)
1	–	0	–	–	239	4.8	35
2	0.23	5.0 ± 0.5	30	30.8 ± 0.3	1409 ± 141	3.6 ± 1.8	121 ± 31
2a[a]	0.23	–	30	–	649 ± 74	8.4 ± 1.4	70 ± 18
3	0.30	3.3 ± 0.2	30	30.2 ± 0.7	755 ± 227	8.4 ± 3.4	95 ± 23
4	0.15	6.4 ± 0.8	30	30.0 ± 1.0	2760 ± 360	2.8 ± 0.5	192 ± 20
5	0.15	6.5 ± 0.4	15	14.9 ± 1.0	893 ± 126	7.1 ± 1.2	124 ± 24
6	0.15	7.3 ± 1.0	22.5	23.4 ± 1.6	1483 ± 143	5.1 ± 0.8	173 ± 4
Human artery reference[b]					2031 ± 4225	4.5 ± 6.2	200 ± 119

[a] Design 2a is identical to 2, but fabricated without thermal annealing.

[b] L'Heureux N et al. Human tissue-engineered blood vessels for adult arterial revascularization. Nat Med 2006; 12(3): 361–5.